NEOPLASIA
www.neoplasia.com

Volume 11 Number 5 May 2009 pp. 448–458 448

The Plasticity of Oncogene Addiction: Implications for Targeted Therapies Directed to Receptor Tyrosine Kinases[1,2]

Vinochani Pillay*, Layal Allaf*,†, Alexander L. Wilding*,†, Jacqui F. Donoghue†, Naomi W. Court†, Steve A. Greenall*,†, Andrew M. Scott* and Terrance G. Johns*,†

*Ludwig Institute for Cancer Research, Heidelberg, Victoria 3084, Australia; †Monash University, Monash Institute of Medical Research, Clayton, Victoria 3168, Australia

Abstract

A common mutation of the epidermal growth factor receptor (EGFR) in glioblastoma multiforme (GBM) is an extracellular truncation known as the de2-7 EGFR (or EGFRvIII). Hepatocyte growth factor (HGF) is the ligand for the receptor tyrosine kinase (RTK) c-Met, and this signaling axis is often active in GBM. The expression of the HGF/c-Met axis or de2-7 EGFR independently enhances GBM growth and invasiveness, particularly through the phosphatidylinositol-3 kinase/pAkt pathway. Using RTK arrays, we show that expression of de2-7 EGFR in U87MG GBM cells leads to the coactivation of several RTKs, including platelet-derived growth factor receptor β and c-Met. A neutralizing antibody to HGF (AMG 102) did not inhibit de2-7 EGFR–mediated activation of c-Met, demonstrating that it is ligand-independent. Therapy for parental U87MG xenografts with AMG 102 resulted in significant inhibition of tumor growth, whereas U87MG.Δ2-7 xenografts were profoundly resistant. Treatment of U87MG.Δ2-7 xenografts with panitumumab, an anti-EGFR antibody, only partially inhibited tumor growth as xenografts rapidly reverted to the HGF/c-Met signaling pathway. Cotreatment with panitumumab and AMG 102 prevented this escape leading to significant tumor inhibition through an apoptotic mechanism, consistent with the induction of oncogenic shock. This observation provides a rationale for using panitumumab and AMG 102 in combination for the treatment of GBM patients. These results illustrate that GBM cells can rapidly change the RTK driving their oncogene addiction if the alternate RTK signals through the same downstream pathway. Consequently, inhibition of a dominant oncogene by targeted therapy can alter the hierarchy of RTKs resulting in rapid therapeutic resistance.

Neoplasia (2009) 11, 448–458

Introduction

The most common malignant neoplasm of the brain is glioblastoma multiforme (GBM), accounting for approximately 25% of brain tumors [1]. GBM is among the most lethal and difficult forms of cancer to treat; thus, the development of novel therapeutic options is critical [1]. At least three key signaling pathways seem to be associated with the development of GBM: the p53, the retinoblastoma protein, and receptor tyrosine kinase (RTK)/*ras*/phosphatidylinositol-3 kinase pathways [2,3]. Activation of phosphatidylinositol-3 kinase is often mediated by signaling from the epidermal growth factor receptor (EGFR) and/or c-Met RTKs [2].

The EGFR has been shown to be activated in GBM by autocrine loop, overexpression, gene amplification, missense mutation, and multiple exon deletion [4–11]. A recent comprehensive analysis of the EGFR demonstrated that, collectively, alterations of the *EGFR* occur in 45% of GBM patients [2]. Including overexpression and functional

Abbreviations: EGFR, epidermal growth factor receptor; GBM, glioblastoma multiforme; HGF, hepatocyte growth factor; PDGFRβ, platelet-derived growth factor receptor β; RTK, receptor tyrosine kinase

Address all correspondence to: Terrance G. Johns, Monash Medical Centre, Monash Institute of Medical Research, 246 Clayton Rd, Clayton 3168 Victoria, Australia.
E-mail: Terry.Johns@med.monash.edu.au

[1]This grant was funded in part by the National Health & Medical Council of Australia (Project Grant 433615) and the James S. McDonnell Foundation Research (no. 220020173).
[2]This article refers to supplementary materials, which are designated by Figures W1 and W2 and are available online at www.neoplasia.com.
Received 24 January 2009; Revised 20 February 2009; Accepted 22 February 2009

DOI 10.1593/neo.09230

autocrine loops in this figure, it is clear that most patients have some activation of the EGFR, supporting a fundamental role for this receptor in the development and progression of GBM. Numerous studies have shown that the most common mutation in GBM is the de2-7 EGFR, occurring in approximately 50% of cases where the *EGFR* gene is amplified [8,10]. However, this estimate might be on the low side because some GBMs only have a low percentage of cells expressing the de2-7 EGFR making it difficult to detect [6]. This cancer-specific *EGFR* mutant has a complete deletion of exons 2 to 7 of *EGFR*. The truncation leads to the elimination of 267 amino acids from the extracellular domain and the insertion of a novel glycine at the fusion junction. This renders the mutant *EGFR* unable to bind any known ligand. Despite this, the de2-7 EGFR is capable of low-level constitutive signaling, which is augmented by the mutant receptor's impaired internalization and down-regulation [12].

The *MET* gene, which encodes the c-Met RTK, is amplified in approximately 4% of GBMs but is only rarely mutated [2]. However, coexpressions of c-Met with its ligand, scatter factor/hepatocyte growth factor (HGF), is often seen in GBM, and this has been shown to correlate with tumor grade [13]. Furthermore, transfection of GBM cells with HGF enhances their tumorigenicity and growth, and the inhibition of HGF or c-Met *in vivo* inhibits tumor formation and cell growth, all indicating that this signaling axis has a key role in this tumor [14,15]. Expression of HGF may also have an indirect role in tumor development through stimulation of angiogenesis, predominantly by activation of vascular endothelial cells [14,15].

Oncogenic addiction is the proposed mechanism by which a tumor cell becomes largely reliant on a single activated oncogene [16,17]. It has also been suggested that oncogene addiction leads to activation of both survival and apoptotic pathways, but in viable tumor cells, the prosurvival signal outweighs the apoptotic signal [18]. Sudden inhibition of this dominant oncogenic signal can lead to oncogenic shock, a scenario where, after withdrawal of the signal, mediators of survival decay faster than those associated with apoptosis, resulting in an excess of proapoptotic signals and cell death [18]. Given their apparent dominant role in some GBM, targeted therapies that inhibit the function of EGFR or c-Met may have antitumor activity in this disease through this mechanism [19,20]. Two such targeted therapies are AMG 102, a fully human antibody directed to HGF/scatter factor currently undergoing clinical evaluation in GBM [21], and panitumumab, a clinically approved fully human antibody directed to the EGFR [22].

The GBM cell line, U87MG, contains a robust c-Met/HGF autocrine loop that strongly drives its proliferation and survival [21]. Therapeutics directed to either HGF or c-Met inhibit the growth of U87MG cells *in vitro* and possess antitumor activity against U87MG xenografts [21,23]. Very recently, it was suggested that the de2-7 EGFR leads to increased phosphorylation of c-Met when coexpressed in U87MG cells [24]. Given this potential interplay between de2-7 EGFR and c-Met, we sought to determine what effect de2-7 EGFR expression has on AMG 102 therapy. Furthermore, we examined the antitumor activity of AMG 102 in combination with panitumumab. Finally, we determined whether the expression of de2-7 EGFR activates other RTKs in GBM cells.

Materials and Methods

Cell Lines and Monoclonal Antibodies

A549 cells were obtained from American Type Tissue Collection (Manassas, VA). The U87MG parental cells and its transfected variants, U87MG.Δ2-7, U87MG.DK, and U87MG.DY5, have been described in detail previously [25]. To ensure the quality of our U87MG-derived cell lines, we routinely produce new transfected cell lines. To guarantee the original characteristics of the parental line are retained, apart from expression of the de2-7 EGFR, cells are not cloned but sorted for the top 10% of de2-7 EGFR–expressing cells. Further precautions include discarding cells after 8 to 12 weeks in culture, always using early-passage freeze downs, and transfection controls. All cell lines were maintained in Dulbecco's modified Eagle's medium/F12 containing 10% fetal calf serum, 2 mM glutamine, and penicillin/streptomycin (Invitrogen, Melbourne, Victoria, Australia). In addition, transfected cell lines were maintained in 400 μg/ml Geneticin (Invitrogen). AMG 102 and panitumumab were provided by Amgen, Inc (Thousand Oaks, CA).

Human Phospho-RTK Arrays

Cells were seeded in complete medium, allowed to attach overnight, and then serum-starved for 18 to 20 hours. The cells were harvested with 0.05% EDTA prepared in PBS, washed twice with ice-cold PBS, and counted. Cells (~1.2×10^7 per treatment) were then lysed and analyzed with human Phospho-RTK arrays (R&D Systems, Minneapolis, MN) as per manufacturer's instructions.

Western Blot Analyses

For the detection of total and phosphorylated c-Met, cells were seeded at a density of 120,000 to 150,000 cells per well in a six-well cell culture plate and were allowed to attach overnight. Cells were washed twice with PBS and once with serum-free medium and then serum-starved in the presence and absence of antibody treatments. Cells were washed twice with ice-cold PBS and lysed by adding Triton X-100 cell lysis buffer [30 mM HEPES, pH 7.4, 150 mM NaCl, 1% Triton X-100, 10 mM NaF, Calbiochem Protease Inhibitor Cocktail Set I, 200 μM Na_3VO_4, and 0.4% (v/v) H_2O_2] and incubating on ice for 20 minutes. The lysates were then clarified by centrifugation at 4°C before immunoprecipitation of c-Met was conducted using the anti–c-Met (C-28) antibody conjugated to agarose beads (Santa Cruz Biotechnology, Santa Cruz, CA).

For the detection of total and phosphorylated de2-7 EGFR, cells were seeded and treated as described above, harvested with trypsin, and washed twice with PBS. Cells were then lysed by resuspending the cell pellet in RIPA buffer [50 mM HEPES, pH 7.4, 150 mM NaCl, 10% (v/v) glycerol, 5 mM EDTA, 1% (v/v) Triton X-100, 1% (v/v) sodium deoxycholate, 0.1% (v/v) SDS, 10 mM NaF, Calbiochem Protease Inhibitor Cocktail Set I, 200 μM Na_3VO_4, and 0.4% (v/v) H_2O_2] and incubated on ice for 5 to 10 minutes. The lysate was clarified by centrifugation at 4°C.

Protein samples were separated on NuPAGE Novex 4% to 12% Bis-Tris Gels (Invitrogen) and transferred to polyvinylidene difluoride membranes using the iBlot Dry Blotting System (Invitrogen). All blocking steps and antibody incubations were performed in Odyssey Blocking Buffer (LI-COR Biosciences, Lincoln, NE). Total c-Met and phosphorylated c-Met was detected by probing with Met (25H2) mouse mAb (Cell Signaling Technology, Danvers, MA) and rabbit (polyclonal) phosphospecific anti–c-Met [$pYpYpY^{1230/1234/1235}$] (Invitrogen), respectively. Total EGFR was detected by probing with mAb 806 (produced in the Biological Production Facility, Ludwig Institute for Cancer Research, Melbourne, Australia), and phosphorylated EGFR was detected with phospho-EGFR (Tyr1173) (53A5) rabbit mAb and phospho-EGFR (Tyr1068) antibody (Cell Signaling Technology). α-Tubulin was detected by probing with α-tubulin (B-7; Santa Cruz

Biotechnology). Secondary antibodies used for detection were either IRDye 800CW–conjugated affinity-purified antirabbit immunoglobulin G (IgG; H&L; Rockland Immunochemicals, Gilbertsville, PA) or Alexa Fluor 680 goat antimouse IgG (H+L; Invitrogen). Western blots were analyzed with the Odyssey Infrared Imaging System (LI-COR Biosciences).

Bio-Plex Assays

Cells were seeded at a density of 200,000 cells per well in six-well cell culture plates and allowed to attach overnight. Cells were washed twice with PBS and once with serum-free medium and then serum-starved in the presence and absence of antibody treatments. The cells were then washed and lysed, and the lysates were analyzed for levels of phosphorylated platelet-derived growth factor receptor β (PDGFRβ) or Akt using the Bio-Plex Phosphoprotein Detection Reagent Kit, Bio-Plex Cell Lysis Kit, Bio-Plex Phosphoprotein Assays (PDGFRβ and Akt), and Bio-Plex Total Target Assays (Akt; Bio-Rad Laboratories, Hercules, CA) according to the manufacturer's protocol.

Xenograft Models

Tumor cells (2×10^6) in 100 μl of growth medium were inoculated subcutaneously into both flanks of 4- to 6-week-old, female BALB/c nude mice (Animal Research Centre, Perth, Australia). All studies were conducted using established tumor models as previously reported [25]. Treatment commenced once tumors had reached a mean volume of 80 to 130 mm^3 and was administered by intraperitoneal (i.p.) injection. Tumor volume in cubic millimeters was determined using the formula (length × width^2) / 2, where length was the longest axis and width was the measurement at right angles to the length. Data are expressed as mean tumor volume ± SEM for each treatment group. All data were analyzed for significance by Student's *t* test. This research project was approved by the Animal Ethics Committee of the Austin Hospital.

Immunohistochemistry

Blood vessels were identified using monoclonal rat antimouse CD31 (5 μg/ml; BD Biosciences Pharmingen, San Jose, CA). Proliferating cells were identified using monoclonal rabbit antimouse Ki67 (1:100 supernatant; Neomarkers, Freemont, CA). Apoptotic cells were identified with a terminal deoxynucleotidyl transferase–mediated dUTP nick end labeling–peroxidase (TUNEL-POD) *in situ* cell death detection kit (Roche Diagnostics, Mannheim, Germany).

For CD31 and Ki67 analysis, frozen sections (6 μm) were fixed in acetone for 5 minutes and washed in PBS for 30 minutes. Sections were incubated with 3% H_2O_2 in methanol for 10 minutes to quench endogenous peroxidase. All sections were incubated with a protein-blocking solution (Dako Australia, Kingsgrove, Australia) to prevent nonspecific binding. Negative controls were performed by replacing the primary antibodies with an isotype-matched IgG control at the same concentration as the primary antibody. The TUNEL-POD was performed according to the manufacturer's instructions. A TUNEL-POD–negative control was prepared by the removal of the primary antibody, whereas the positive control was prepared by incubating sections with a DNAse/Tris solution according to the manufacturer's instructions (10 minutes at 24°C) before incubating with the primary antibody. In all cases, incubation with primary antibody was 1 hour at room temperature.

Anti-CD31 was visualized with an antirat biotinylated antibody for 1 hour (1:200; Invitrogen) followed by LSAB-2 HRP (15 min; Dako Australia) and color development with the chromogen 3,30-diaminobenzidine (Sigma Aldrich, St. Louis, MO). Anti-Ki67 was visualized with Envision antirabbit–HRP (30 minutes; Dako Australia) followed by aminoethyl carbazole (Invitrogen). The TUNEL immunostains were incubated with the POD converter antibody (1 hour at 37°C) and visualized with 3,30-diaminobenzidine.

All image analyses were performed using the Analytical Imaging System (AIS 30, Rev 1.7; Imaging Research Inc. GE Healthcare Bio-Sciences, Rydalmere, NSW, Australia). Positive cells or vessels were counted from six fields of view, results were presented as mean values ± SEM, and statistical tests were performed using the Statistical Package for the Social Sciences for Windows, version 15.1 (SPSS, Inc, Chicago, IL). Data were analyzed using one-way analysis of variance followed by Tukey's *post hoc* tests and Student's *t* test for individual mean analysis. $P < .05$ was considered significant.

Results

Coactivation of RTKs in Glioma Cells Expressing the de2-7 EGFR

To identify cell surface RTKs potentially activated by the de2-7 EGFR, whole-cell lysates from U87MG.Δ2-7 and U87MG.DK cell lines were analyzed using a human phospho-RTK antibody array. Multiple RTKs were shown to be coactivated in U87MG.Δ2-7 glioma cells expressing the constitutively active de2-7 EGFR compared with U87MG.DK cells expressing the kinase dead de2-7 EGFR (Figure 1*A*), including c-Met, PDGFRβ, vascular endothelial growth factor receptor 3, EphA7, fibroblast growth factor receptor 3, and Axl. This coactivation observed by antibody array was confirmed for two of the RTKs: c-Met by Western blot (Figure 1*B*) and PDGFRβ by Bio-Plex (Figure 1*C*). We repeated the array experiment with an independent U87MG.Δ2-7 cell line derived earlier and obtained near-identical results. Thus, expression of the de2-7 EGFR leads to activation of several cell surface RTKs.

Effect of Inhibiting the de2-7 EGFR on Activation of RTKs and Akt

To determine the effect of panitumumab (an anti-EGFR antibody) on de2-7 EGFR activation, the receptor from U87MG.Δ2-7 cells treated with this antibody was analyzed for its phosphorylation status at two of the major autophosphorylation sites (Y1086 and Y1173). The level of phosphorylation at Y1086 and Y1173 was greatly reduced with panitumumab treatment, indicating that this antibody inhibits phosphorylation of the de2-7 EGFR (Figure 2*A*). Analysis of total receptor levels showed that panitumumab partially downregulated the receptor, although the effect was smaller than that seen on phosphorylation. These findings demonstrate that panitumumab inhibits the de2-7 EGFR.

Given that a recent study has shown that the de2-7 EGFR drives ligand-independent phosphorylation of c-Met [24], the effect of AMG 102 (a neutralizing anti-HGF antibody) or panitumumab on c-Met phosphorylation was examined by Western blot analysis. Figure 2*B* shows that c-Met is robustly phosphorylated in U87MG.Δ2-7 cells even in the presence of AMG 102. In contrast, treatment of U87MG.Δ2-7 cells with panitumumab resulted in a profound decrease in c-Met phosphorylation (Figure 2*B*). As expected, combination treatment with panitumumab and AMG 102 also fully inhibited the phosphorylation of c-Met. Thus, activated de2-7 EGFR drives c-Met phosphorylation in an HGF-independent fashion.

The effect of panitumumab on another de2-7 EGFR–activated RTK, PDGFRβ, was also tested. Lysates from untreated U87MG.Δ2-7 cells, as well as cells treated with AMG 102, panitumumab, or a combination

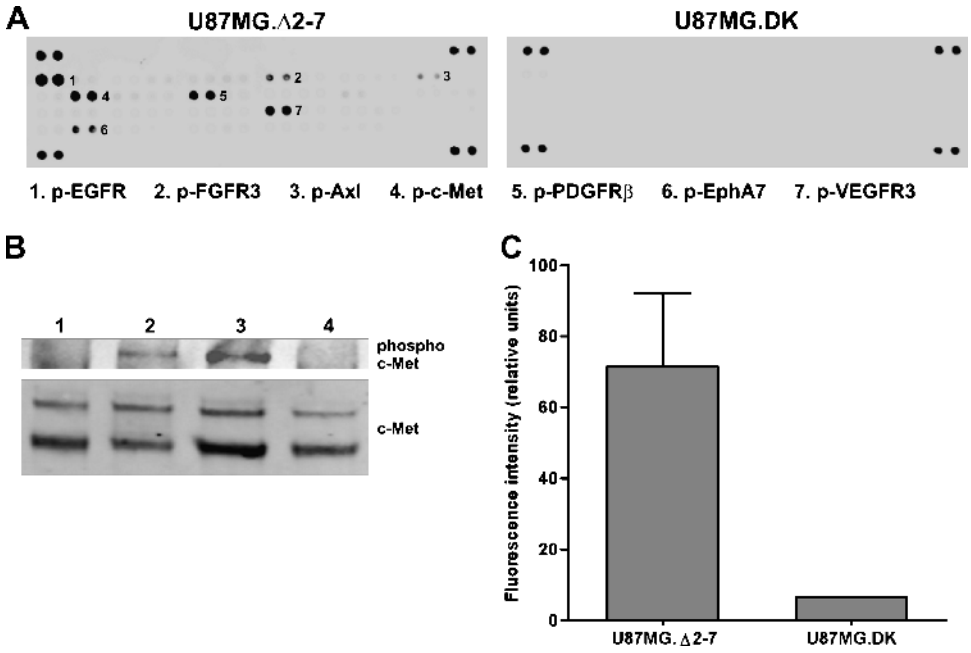

Figure 1. Coactivation of RTKs by de2-7 EGFR in U87MG cell lines. (A) RTK antibody arrays were used to compare RTK activation in glioma cells expressing the de2-7 EGFR (U87MG.Δ2-7) or dead kinase de2-7 EGFR (U87MG.DK). The identity of phosphorylated RTKs is indicated by number. (B) Western blot analysis showing levels of phosphorylated and total c-Met in U87MG cells (lane 1), U87MG cells stimulated with HGF (lane 2), U87MG.Δ2-7 cells (lane 3), and U87MG.DK cells (lane 4). (C) Comparison of phosphorylated PDGFRβ in U87MG.Δ2-7 and U87MG.DK cell lines as determined by Bio-Plex assay. All assays performed a minimum of three times.

of both, were analyzed by Bio-Plex to determine the degree of phosphorylation of PDGFRβ. Treatment with AMG 102 yielded only a small reduction in PDGFRβ phosphorylation, whereas treatment with panitumumab resulted in a profound decrease in PDGFRβ phosphorylation (Figure 2*C*). Combination treatment with panitumumab and AMG 102 had resulted in inhibition similar to panitumumab alone. Therefore, de2-7 EGFR also mediates phosphorylation of PDGFRβ.

The effect of panitumumab and AMG 102 on activation of Akt, a major downstream target of the EGFR and c-Met signaling pathways, was examined using Bio-Plex [26]. Treatment of U87MG.Δ2-7 cells with AMG 102 caused no reduction in Akt phosphorylation (pAkt), whereas treatment with panitumumab resulted in complete inhibition of pAkt (Figure 2*D*). Not surprisingly, combination treatment with panitumumab and AMG 102 also completely inhibited pAkt (Figure 2*D*). As anticipated, U87MG.DK cells had much lower levels of basal pAkt (cf., the scales in Figure 2*E* with Figure 2*D*) because of the absence of a functional de2-7 EGFR. Treatment of U87MG.DK cells with AMG 102 yielded a substantial decrease in pAkt (Figure 2*E*), demonstrating that AMG 102 does inhibit c-Met signaling in U87MG-derived cells lacking a functional de2-7 EGFR. Treatment of U87MG.DK cells with panitumumab reduced pAkt compared with untreated cells (Figure 2*E*), suggesting that at least some of the pAkt is generated by the wild-type EGFR that is coexpressed in these cells. Combination treatment with both antibodies did not have any additional effects on pAkt compared with AMG 102 treatment alone (Figure 2*E*). The levels of total Akt in the U87MG.Δ2-7 cells were not significantly changed by any of the antibody treatments (Figure 2*F*); however, panitumumab alone and in combination with AMG 102 reduced the level of total Akt in U87MG.DK cells (Figure 2*G*). This reduction was less than the reduction in pAkt. Thus, AMG 102 is unable to inhibit pathways downstream of c-Met when de2-7 EGFR is coexpressed.

Treatment of Established Glioma Xenografts with Panitumumab and AMG 102

U87MG and U87MG.Δ2-7 glioblastoma xenografts were treated with AMG 102 to determine whether the de2-7 EGFR reduces efficacy of AMG 102 treatment. Treatment of established U87MG xenografts with 30 μg of AMG 102, twice a week for 2 weeks, produced a significant antitumor response (Figures 3*A* and W1). The average tumor volumes on day 49 after inoculation were 1580 and 260 mm^3 ($P < .0001$) for the vehicle and AMG 102 treatment groups, respectively. Two of the 16 tumors in the AMG 102 group showed complete regression; histological examination of two other tumors that had regressed showed only small clusters of remaining tumor cells. In contrast, U87MG.Δ2-7 xenografts were relatively resistant to AMG 102 therapy (Figure 3*B*). The average tumor volumes on day 19 after inoculation were 1820 and 1360 mm^3 ($P = .02$) for the vehicle and AMG 102 treatment groups, respectively. This result indicates that the expression of de2-7 EGFR causes significant resistance to AMG 102. U87MG.wt xenografts, which overexpress the wild-type EGFR to a similar level as de2-7 EGFR in U87MG.Δ2-7 cells, were treated with AMG 102 to determine whether this receptor also influences the efficacy of AMG 102. Treatment of established U87MG.wt xenografts with AMG 102 produced a significant antitumor response comparable to that observed in the parental xenografts (Figure 3*C*). The average tumor volumes on day 47 after inoculation were 1400 and 250 mm^3 ($P < .0001$) for the vehicle and AMG 102 treatment groups, respectively. This result indicates that overexpression of the wild-type EGFR does not mediate resistance to AMG 102.

U87MG.Δ2-7 xenografts were then treated with a combination of panitumumab and AMG 102 and each of the antibodies alone to determine whether panitumumab reverses the resistance mediated by the de2-7 EGFR (Figures 3*D* and W1). Tumors in all three antibody-treated groups were significantly smaller than in the vehicle-treated

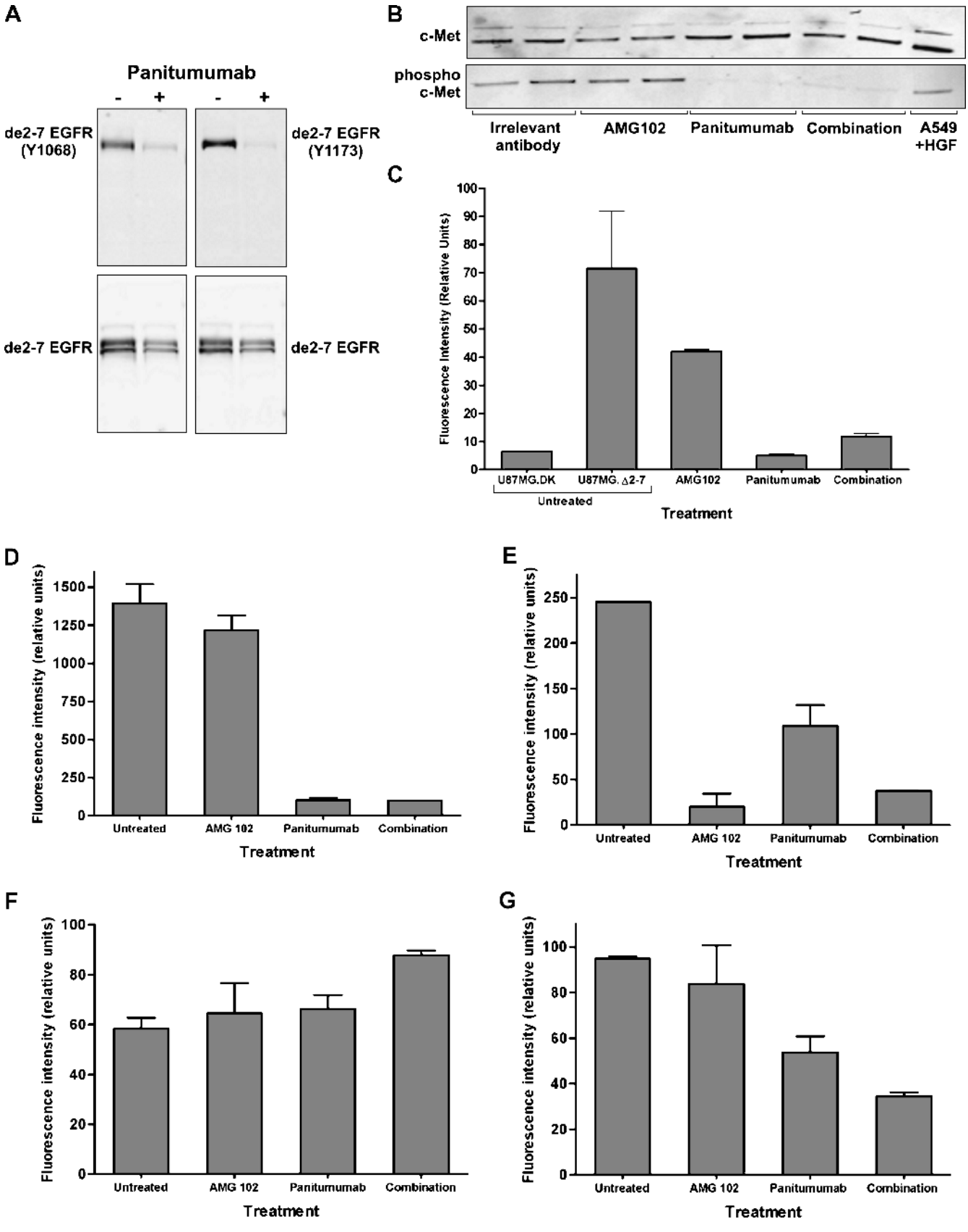
A
Panitumumab
- + - +
de2-7 EGFR (Y1068)
de2-7 EGFR (Y1173)
de2-7 EGFR
de2-7 EGFR
B
c-Met
phospho c-Met
Irrelevant antibody
AMG102
Panitumumab
Combination
A549 +HGF
C
Fluorescence Intensity (Relative Units)
U87MG.DK
U87MG.Δ2-7
AMG102
Panitumumab
Combination
Untreated
Treatment
D
Fluorescence intensity (relative units)
Untreated
AMG 102
Panitumumab
Combination
Treatment
E
Fluorescence intensity (relative units)
Untreated
AMG 102
Panitumumab
Combination
Treatment
F
Fluorescence intensity (relative units)
Untreated
AMG 102
Panitumumab
Combination
Treatment
G
Fluorescence intensity (relative units)
Untreated
AMG 102
Panitumumab
Combination
Treatment

group at day 19 after inoculation. The mean tumor volumes were 1820, 1360, 570, and 170 mm^3 for the vehicle, AMG 102 ($P = .02$), panitumumab ($P < .0001$), and combination ($P < .0001$) treatment groups, respectively (Figure 3*D*). The combination of panitumumab and AMG 102 resulted in the greatest antitumor activity and was significantly more efficacious than the panitumumab-alone group ($P = .0008$ at day 26 after inoculation). Thus, panitumumab reversed the resistance to AMG 102 mediated by the de2-7 EGFR resulting in greater than additive antitumor activity.

To determine whether the resistance of U87MG.Δ2-7 xenografts to AMG 102 could be overcome by using a higher dose of the antibody, we repeated the above experiment using a dose of 100 μg of AMG 102 twice a week for 2 weeks (Figure 3*E*). The average tumor volumes on day 21 after inoculation were 2150, 1530, 780, and 150 mm^3 for the vehicle, AMG 102, panitumumab, and combination treatment groups, respectively (Figure 3*E*). Treatment with the higher dose of AMG 102 resulted in a small inhibition of tumor growth ($P = .03$), but it failed to overcome the resistance mediated by the de2-7 EGFR. Once again, the combination of high-dose AMG 102 with panitumumab was more effective than either agent alone; however, the antitumor activity was similar to that seen at the lower dose of AMG 102 (cf., Figure 3*D*).

Mechanism of Antitumor Activity

To elucidate the antitumor mechanisms of panitumumab and AMG 102, we conducted an immunohistochemical analysis on U87MG.Δ2-7 xenografts harvested from mice killed mid treatment (1 day after the second injection). This time point was chosen to determine the primary effects of treatment. Mice were treated with vehicle, AMG 102, panitumumab, or the combination of these two antibodies as described above for Figure 3*D*. To determine whether antibody treatment had an antiproliferative effect on xenografts, we analyzed the number of Ki67-positive cells, a marker for proliferating cells. There was no significant difference in the number of Ki67-positive cells per field of view ($P = .201$) among the treatment groups (Figure 4, *A* and *B*).

The microvessel density of treated U87MG.Δ2-7 xenografts was assessed by immunostaining sections for CD31 (Figure 4, *C* and *D*). The average number of CD31-positive microvessels per field of view was 47, 42, 33, and 42 for the vehicle, panitumumab, AMG 102, and combination treatment groups, respectively. The AMG 102 treatment group had significantly fewer CD31-positive vessels compared with the other groups ($P = .004$), indicating that AMG 102 treatment was able to restrict intratumoral vasculature development. Treatment with panitumumab alone or in combination with AMG 102 had no effect on tumor vessel density.

The effect of antibody treatment on tumor apoptosis was examined in U87MG.Δ2-7 xenografts using the TUNEL-POD method. The average number of cells staining positive for TUNEL per field of view was 0.5, 19, 1, and 30 for the vehicle, panitumumab, AMG 102, and combination treatment groups, respectively (Figure 4, *E* and *F*). Both the panitumumab and combination therapy groups showed a significant increase in apoptosis compared with vehicle-treated xenografts ($P = .047$ and $P = .012$, respectively). Apoptosis in the combination group was higher than that in the panitumumab group, but this did not reach statistical significance ($P = .29$). However, this result was based on the analysis of the whole tumor section and, therefore, may be an underestimate of the difference between the two groups because the enhancement of apoptosis seen in the combination therapy group was mostly restricted to the central regions of the tumor (Figure 4*F*). We were unable to stain sections for phospho–c-Met because all three antibodies used showed cross-reactivity with the de2-7 EGFR (Figure W2).

Role of de2-7 EGFR Autophosphorylation in Resistance to AMG 102 Therapy

To further assess the mechanism by which de2-7 EGFR interacts with c-Met and causes resistance to AMG 102, we treated animals bearing U87MG.DY5 xenograft tumors with this antibody. This DY5 version of the de2-7 EGFR is unable to autophosphorylate at the five major autophosphorylation sites associated with signaling (Y1173, Y1148, Y1086, Y1068, and Y992 have been changed to phenylalanine) but retains an active kinase domain. Figure 5*A* confirms this lack of phosphorylation at two of the major sites, Y1068 and Y1173. Whereas U87MG.DY5 xenografts grew more slowly than U87MG.Δ2-7 xenografts, the difference was smaller than previously reported. Earlier studies were conducted using intracranial tumors initiated by a low cell number (5×10^3). Current xenografts were grown subcutaneously using considerably more cells (2×10^6); both of these changes partially mask the growth advantage of the de2-7 EGFR.

Treatment of established U87MG.DY5 xenografts with 30 μg of AMG 102, twice a week for 2 weeks, yielded no response to AMG 102 therapy compared with treatment with vehicle (Figures 5*B* and W1). The average tumor volumes on day 21 after inoculation were 1800 and 1950 mm^3 ($P = .67$) for the vehicle and AMG 102 treatment groups, respectively. Thus, the DY5 version of the de2-7 EGFR also causes profound resistance to AMG 102, suggesting that an active kinase but not autophosphorylation is required for the activation of c-Met.

Figure 2. Effect of panitumumab treatment on the phosphorylation of de2-7 EGFR, c-Met, PDGFRβ and Akt. (A) Western blot analysis of cell lysates from U87MG.Δ2-7 cells treated with 20 μg/ml panitumumab showing its effect on de2-7 EGFR at two major autophosphorylaton sites, Y1068 and Y1173 (upper panels), and total de2-7 EGFR (lower panels). Cell lysates from untreated cells served as a baseline control. The faint band seen above the de2-7 EGFR doublet in the lower panels is the wild-type EGFR, which is coexpressed in these cells. (B) Western blot analysis of cell lysates from U87MG.Δ2-7 cells treated with either 10 μg/ml AMG 102, 20 μg/ml panitumumab, or a combination of both showing the effect of these treatments on total c-Met (upper panel) or c-Met phosphorylation (lower panel). Cell lysates from U87MG.Δ2-7 cells treated with an irrelevant antibody served as a negative control, whereas lysates from A549 cells stimulated by HGF were used as a positive control. (C) Bio-Plex analysis of cell lysates from U87MG.Δ2-7 cells treated with either 10 μg/ml AMG 102, 10 μg/ml panitumumab, or a combination of these antibodies to determine their effect on phosphorylation of PDGFRβ. Untreated U87MG.Δ2-7 and U87MG.DK cell lysates are included for baseline. (D–G) Bio-Plex analysis of cell lysates from U87MG.Δ2-7 (D and F) and U87MG.DK (E and G) cells treated with either 10 μg/ml AMG 102, 10 μg/ml panitumumab, or a combination of these antibodies to determine the effect of these treatments on total (F and G) and phosphorylated Akt (D and E).

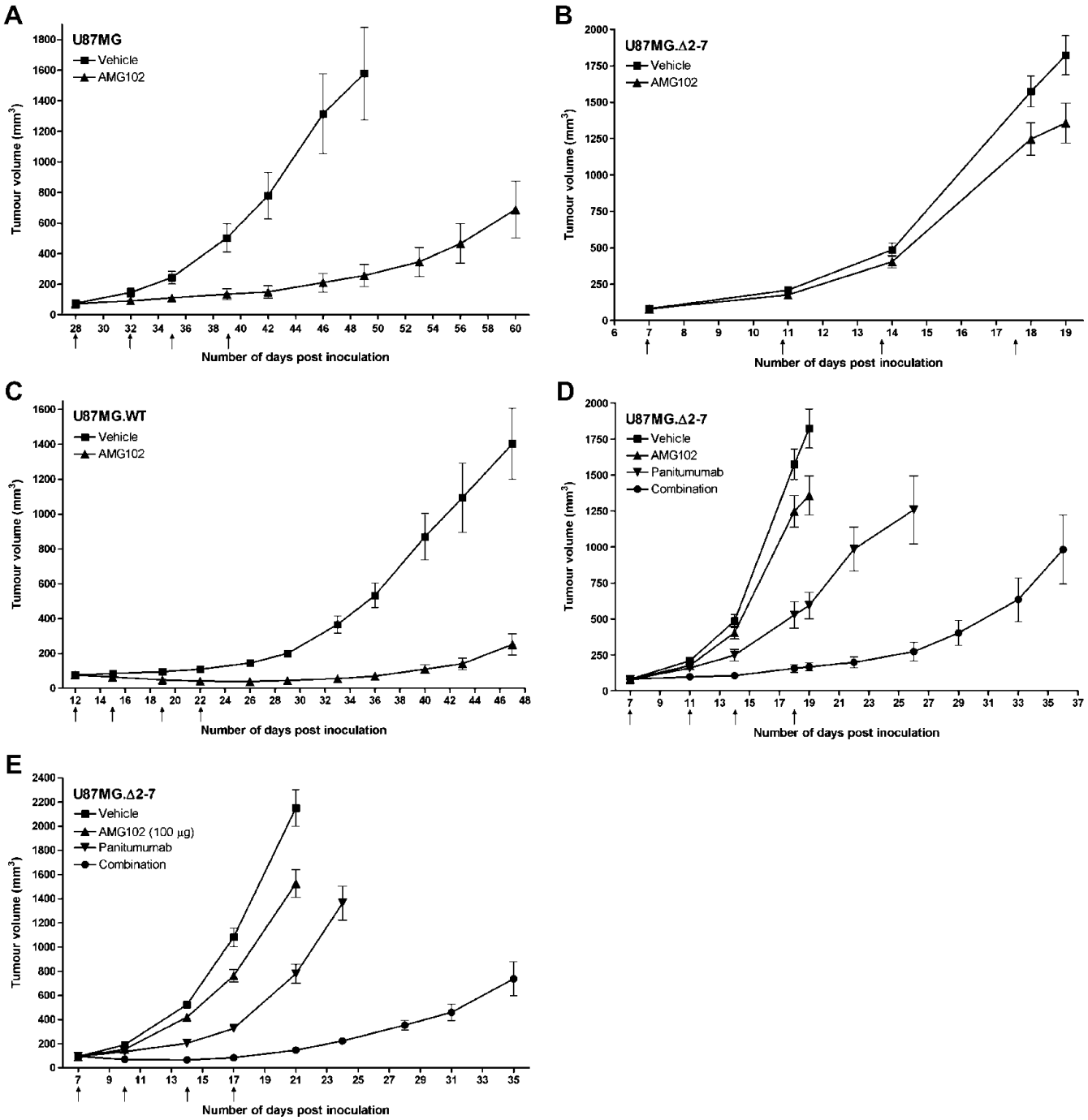

Figure 3. Treatment of established glioma xenografts with panitumumab and AMG 102. (A) Mice bearing two U87MG xenografts per mouse were injected i.p. with PBS (n = 7) or 30 μg of AMG 102 (n = 8), twice weekly for 2 weeks once average tumor volumes had reached 80 mm^3. (B) Mice (n = 6) bearing U87MG.Δ2-7 xenografts were injected i.p. as described in (A). (C) Mice (n = 7) bearing U87MG.wt xenografts were injected i.p. as described in (A). (D) Mice bearing U87MG.Δ2-7 xenografts were injected i.p. with PBS (n = 6), 30 μg of AMG 102 (n = 6), 1 mg of panitumumab (n = 5), or a combination of both these antibodies (n = 5), twice weekly for 2 weeks once average tumor volumes had reached 80 mm^3. (E) Mice bearing U87MG.Δ2-7 xenografts were injected i.p. with PBS (n = 7), 100 μg of AMG 102 (n = 7), 1 mg of panitumumab (n = 5), or a combination of both these antibodies (n = 5), twice weekly for 2 weeks once average tumor volumes had reached 90 mm^3. Arrows indicate days on which i.p. injections were administered; n = number of mice per treatment group. Data were expressed as mean tumor volume ± SEM.

Discussion

Cross talk between the EGFR and c-Met in tumor cells was first reported by Jo et al. [27], who showed that the activation of c-Met in several transformed cell lines was mediated by the EGFR ligand transforming growth factor α. This interaction was proposed to be unidirectional, but at least one recent report has shown that overexpression of c-Met can also result in the activation of EGFR [28]. A recent phosphoproteomics screen identified c-Met as a phosphorylated protein expressed in U87MG.Δ2-7 cells [24]. One difficulty with this study is that some of the confirmatory Western blot analyses

were performed using whole-cell lysates, and because phospho–c-Met antibodies cross-react with phosphorylated de2-7 EGFR, these Western blots need to be interpreted with caution (Figure W2). Our RTK screen shows that the expression of de2-7 EGFR in U87MG glioma cells leads to phosphorylation of c-Met, a result we confirmed by immunoprecipitation/Western analysis. The absence of c-Met phosphorylation in cells expressing a dead kinase version of de2-7 EGFR demonstrates that the receptor needs to be kinase active. Because incubation of U87MG.Δ2-7 cells with AMG 102 failed to inhibit the phosphorylation of c-Met, this activation must be HGF-independent. In

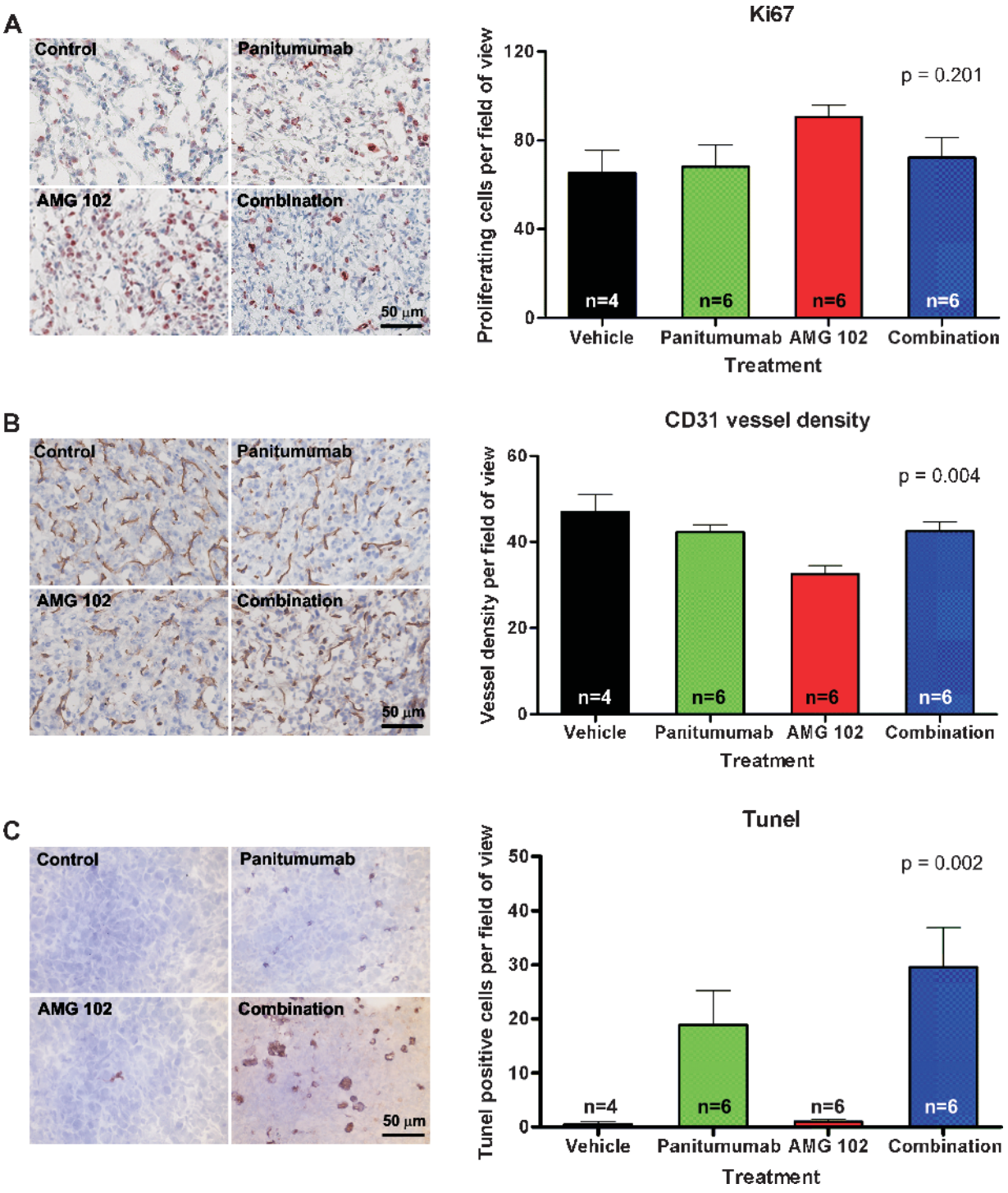

Figure 4. Immunohistochemical analyses of U87MG.Δ2-7 xenografts treated with AMG 102, panitumumab, or a combination of these antibodies. Mice with established U87MG.Δ2-7 xenografts (120 mm^3) were treated with PBS, 1 mg of panitumumab, 30 μg of AMG 102, and a combination of panitumumab and AMG 102 on days 7 and 10 after inoculation and tumors resected on day 11. Frozen sections from individual tumors from each treatment group were stained for Ki67 (proliferation marker, A), CD31 (vessel marker, B), and TUNEL (apoptosis marker, C). The number of cells/vessels staining positive per field of view (original magnification, ×200) was calculated for each marker, and data were expressed as mean number of cells/vessels per field ± SEM, n = number of fields counted.

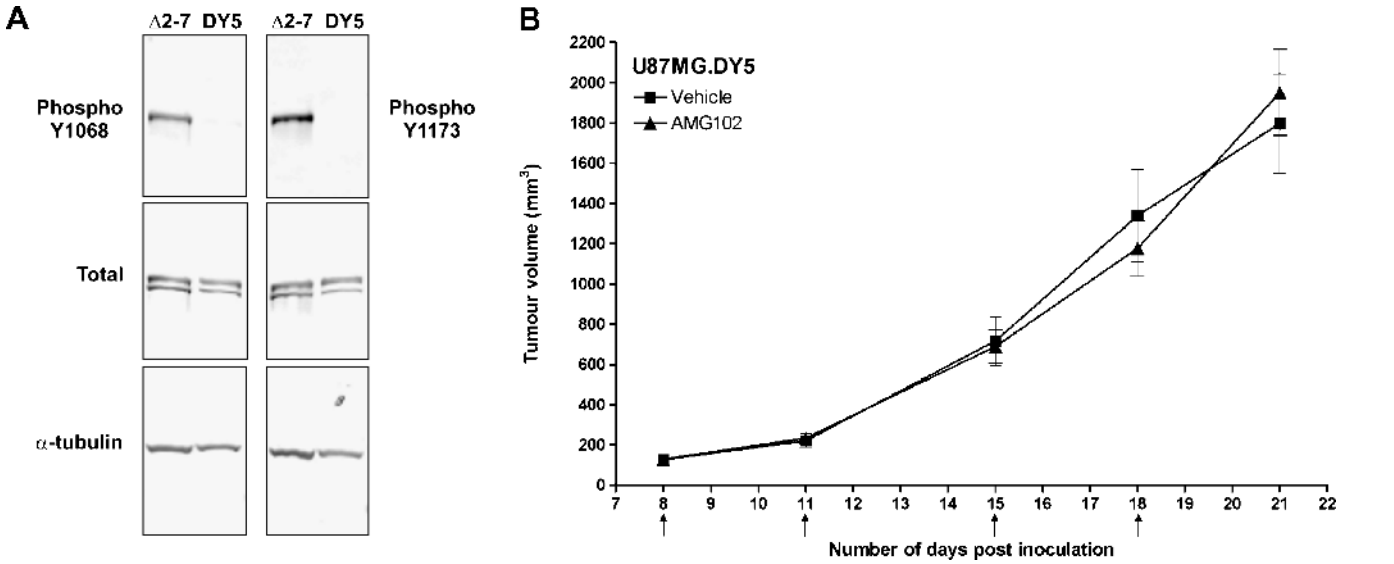

Figure 5. Efficacy of AMG 102 treatment on U87MG.DY5 xenografts. (A) Western blot analysis of cell lysates from U87MG.Δ2-7 and U87MG.DY5 cells showing phosphorylation status at the Y1068 and Y1173 autophosphorylation sites (upper panels), total de2-7 EGFR or DY5 (middle panels), and α-tubulin as a loading control (lower panels). (B) Mice (n = 6) bearing U87MG.DY5 xenografts were injected i.p. with PBS or 30 μg of AMG 102 twice weekly for 2 weeks once average tumor volumes had reached 130 mm^3. Arrows indicate days on which i.p. injections were administered; n = number of mice per treatment group. Data were expressed as mean tumor volume ± SEM.

contrast, treatment of U87MG.Δ2-7 cells with panitumumab, which binds and inhibits de2-7 EGFR phosphorylation, ablated the phosphorylation of c-Met, further confirming that c-Met activation is mediated by de2-7 EGFR.

Phosphorylation of Akt is downstream of both de2-7 EGFR and c-Met [29,30]. Addition of AMG 102 to U87MG.DK cells reduced the level of pAkt as expected. Interestingly, pAkt was also reduced by panitumumab, suggesting that the endogenous wild-type EGFR also contributes to pAkt in these cells. Expression of de2-7 EGFR in U87MG cells dramatically enhanced pAkt levels, this increase being reversible by treatment with panitumumab. In contrast, AMG 102 had virtually no effect on the level of pAkt in U87MG.Δ2-7 cells, confirming the inability of this HGF-neutralizing antibody to reduce c-Met–stimulated pAkt in cells expressing de2-7 EGFR. This lack of *in vitro* response to AMG 102 was extended to tumor models, where low-dose AMG 102 had profound antitumor activity against U87MG and U87MG.wt xenografts but only a minor effect on the growth of U87MG.Δ2-7 xenografts, even at high doses. In contrast, panitumumab inhibited the growth of U87MG.Δ2-7 xenografts by inducing apoptosis rapidly after the commencement of treatment, consistent with the induction of oncogenic shock. Importantly, the combination of AMG 102 and panitumumab generated greater than additive antitumor activity in U87MG.Δ2-7 xenografts and further increased apoptosis, especially in the central core of the tumor. We are currently screening cells and tumors in an attempt to identify those apoptotic molecules responsible for this antitumor effect [31]. U87MG.DY5 xenografts, which express a de2-7 EGFR molecule with an active kinase but is incapable of autophosphorylation at the five major autophosphorylation sites, were also resistant to AMG 102, suggesting that activation of c-Met by de2-7 EGFR occurs through a direct interaction rather than through phosphorylated docking sites.

Although it is difficult to detect the low level of phosphorylated c-Met in parental U87MG cells (phospho–c-Met is detectable upon overexposure of Western blots), these cells are addicted to oncogenic signals generated by the HGF/c-Met autocrine loop as treatment with AMG 102 leads to complete tumor regressions (Figure 3*A* and [21]). Forced expression of de2-7 EGFR in these cells seems to shift the oncogene addiction from this autocrine loop to the de2-7 EGFR. The ease with which this is achieved probably reflects that de2-7 EGFR and c-Met activate a number of downstream pathways in common, particularly pAkt [29,30]. However, despite the long-term expression of de2-7 EGFR, U87MG.Δ2-7 cells can quickly revert to dependence on the c-Met axis after the antibody-mediated *in vivo* inhibition of de2-7 EGFR. The addition of AMG 102 to the treatment regimen clearly disrupts this process leading to profound tumor inhibition. The plasticity of oncogene addiction demonstrated here has significant implications for targeted therapy. Indeed, our work suggests that some tumor cells can harbor a hierarchy of activated oncogenes, possibly arising through their ongoing evolution. Thus, even targeting of the dominant oncogene in some solid tumors may be relatively ineffective as its inhibition can be rapidly overcome by the promotion of other activated oncogenes to the dominant position within the cell. This provides another reason for the targeting of multiple RTKs or downstream signals to obtain inhibition of GBM growth.

Interestingly, our screen identified several other RTKs potentially activated by de2-7 EGFR, including PDGFRβ. Using an immunofluorescence-based bead assay, we were able to confirm the activation of PDGFRβ by de2-7 EGFR. Thus, our observations may apply to a range of ligand-based therapeutics. Ligand stimulation of the wild-type EGFR can also activate PDGFRβ in a ligand-independent manner by heterodimerization, highlighting that these two classes of receptors can directly interact [32]. Furthermore, PDGFRβ has been shown to drive oncogene addiction in glioma models; thus, it would be interesting to determine the contribution of activated PDGFRβ to the tumorigenicity of de2-7 EGFR [33]. Given the low level of autoactivation seen in the de2-7 EGFR, this promiscuous activation of other RTKs by this receptor may explain its significant protumor activity and possibly why it signals in a qualitatively different manner to the wild-type EGFR [30,34]. We are currently developing phosphorylation assays for EphA7 and fibroblast growth factor receptor 3 to confirm their activation by

de2-7 EGFR. Our initial investigations suggest that it may be EphA2 that is activated not EphA7, once again highlighting issues of uncharacterized antibody cross-reactivity.

Apart from the specific effects on AMG 102 therapy, the promiscuous nature of de2-7 EGFR signaling raises some general questions with respect to the use of targeted therapies. Firstly, using U87MG-transfected cells and relevant controls meant we knew that de2-7 EGFR was the dominant kinase and that the c-Met axis would most likely replace this pathway in U87MG.Δ2-7 xenografts, but identification of the dominant kinase without prior knowledge remains problematical. Secondly, if it is not possible to identify the dominant activated kinase, can you inhibit tumor growth by targeting several of the secondary kinases, and if so, how many need to be functionally blocked? Satisfying answers to these questions would allow for personalized therapeutics that may well improve clinical outcome. Clearly, the ongoing development of targeted therapies needs to be supported by a rigorous analysis of signaling pathways in cell lines and clinical samples so that we can develop methodologies for addressing these questions.

The data presented here will be used to support the initiation of a clinical trial in GBM patients using the combination of panitumumab and AMG 102. The frequent activation of both signaling cascades in GBM and the ability of de2-7 EGFR, and possibly other EGFR mutations, to directly activate c-Met clearly justify such a trial. A variety of EGFR antibodies have been shown to cross the blood-brain barrier, with some efficacy reported [35]. A phase 2 trial with AMG 102 in GBM patients produced clinical responses [36], indicating that this antibody also crosses the blood-brain barrier. Given that bevacizumab, an antibody directed to vascular endothelial growth factor, has shown antitumor activity in GBM models and patients [37,38], it would be interesting to see if it enhances the activity of the panitumumab/AMG 102 combination.

More generally, our observations demonstrate that some tumor cells may contain a hierarchy of activated oncogenes, thus allowing for rapid compensation after the inactivation of the dominant oncogene. The ease by which this occurs raises challenges for targeted therapy approaches not only for GBM but also for other complex solid tumors.

Acknowledgments

The authors thank Terri Burgess, Angela Coxen, and Kelly Oliner (Amgen Inc.) for their helpful advice during this project.

References

[1] Wen PY and Kesari S (2008). Malignant gliomas in adults. *N Engl J Med* **359**, 492–507.

[2] Cancer Genome Atlas Research Network (2008). Comprehensive genomic characterization defines human glioblastoma genes and core pathways. *Nature* **455**, 1061–1068.

[3] Parsons DW, Jones S, Zhang X, Lin JC, Leary RJ, Angenendt P, Mankoo P, Carter H, Siu IM, Gallia GL, et al. (2008). An integrated genomic analysis of human glioblastoma multiforme. *Science* **321**, 1807–1812.

[4] Ekstrand AJ, James CD, Cavenee WK, Seliger B, Pettersson RF, and Collins VP (1991). Genes for epidermal growth factor receptor, transforming growth factor alpha, and epidermal growth factor and their expression in human gliomas *in vivo*. *Cancer Res* **51**, 2164–2172.

[5] Frederick L, Wang XY, Eley G, and James CD (2000). Diversity and frequency of epidermal growth factor receptor mutations in human glioblastomas. *Cancer Res* **60**, 1383–1387.

[6] Jungbluth AA, Stockert E, Huang HJ, Collins VP, Coplan K, Iversen K, Kolb D, Johns TJ, Scott AM, Gullick WJ, et al. (2003). A monoclonal antibody recognizing human cancers with amplification/overexpression of the human epidermal growth factor receptor. *Proc Natl Acad Sci USA* **100**, 639–644.

[7] Libermann TA, Nusbaum HR, Razon N, Kris R, Lax I, Soreq H, Whittle N, Waterfield MD, Ullrich A, and Schlessinger J (1985). Amplification, enhanced expression and possible rearrangement of EGF receptor gene in primary human brain tumours of glial origin. *Nature* **313**, 144–147.

[8] Pedersen MW, Meltorn M, Damstrup L, and Poulsen HS (2001). The type III epidermal growth factor receptor mutation. Biological significance and potential target for anti-cancer therapy. *Ann Oncol* **12**, 745–760.

[9] Sugawa N, Ekstrand AJ, James CD, and Collins VP (1990). Identical splicing of aberrant epidermal growth factor receptor transcripts from amplified rearranged genes in human glioblastomas. *Proc Natl Acad Sci USA* **87**, 8602–8606.

[10] Wikstrand CJ, Reist CJ, Archer GE, Zalutsky MR, and Bigner DD (1998). The class III variant of the epidermal growth factor receptor (EGFRvIII): characterization and utilization as an immunotherapeutic target. *J Neurovirol* **4**, 148–158.

[11] Wong AJ, Bigner SH, Bigner DD, Kinzler KW, Hamilton SR, and Vogelstein B (1987). Increased expression of the epidermal growth factor receptor gene in malignant gliomas is invariably associated with gene amplification. *Proc Natl Acad Sci USA* **84**, 6899–6903.

[12] Schmidt MH, Furnari FB, Cavenee WK, and Bogler O (2003). Epidermal growth factor receptor signaling intensity determines intracellular protein interactions, ubiquitination, and internalization. *Proc Natl Acad Sci USA* **100**, 6505–6510.

[13] Abounader R and Laterra J (2005). Scatter factor/hepatocyte growth factor in brain tumor growth and angiogenesis. *Neuro Oncol* **7**, 436–451.

[14] Benvenuti S and Comoglio PM (2007). The MET receptor tyrosine kinase in invasion and metastasis. *J Cell Physiol* **213**, 316–325.

[15] Gentile A, Trusolino L, and Comoglio PM (2008). The Met tyrosine kinase receptor in development and cancer. *Cancer Metastasis Rev* **27**, 85–94.

[16] Weinstein IB and Joe A (2008). Oncogene addiction. *Cancer Res* **68**, 3077–3080; discussion 3080.

[17] Weinstein IB and Joe AK (2006). Mechanisms of disease: oncogene addiction—a rationale for molecular targeting in cancer therapy. *Nat Clin Pract Oncol* **3**, 448–457.

[18] Sharma SV, Fischbach MA, Haber DA, and Settleman J (2006). "Oncogenic shock": explaining oncogene addiction through differential signal attenuation. *Clin Cancer Res* **12**, 4392s–4395s.

[19] Comoglio PM, Giordano S, and Trusolino L (2008). Drug development of MET inhibitors: targeting oncogene addiction and expedience. *Nat Rev Drug Discov* **7**, 504–516.

[20] Gazdar AF, Shigematsu H, Herz J, and Minna JD (2004). Mutations and addiction to EGFR: the Achilles "heal" of lung cancers? *Trends Mol Med* **10**, 481–486.

[21] Burgess T, Coxon A, Meyer S, Sun J, Rex K, Tsuruda T, Chen Q, Ho SY, Li L, Kaufman S, et al. (2006). Fully human monoclonal antibodies to hepatocyte growth factor with therapeutic potential against hepatocyte growth factor/c-Met–dependent human tumors. *Cancer Res* **66**, 1721–1729.

[22] Rivera F, Vega-Villegas ME, Lopez-Brea MF, and Marquez R (2008). Current situation of panitumumab, matuzumab, nimotuzumab and zalutumumab. *Acta Oncol* **47**, 9–19.

[23] Martens T, Schmidt NO, Eckerich C, Fillbrandt R, Merchant M, Schwall R, Westphal M, and Lamszus K (2006). A novel one-armed anti–c-Met antibody inhibits glioblastoma growth *in vivo*. *Clin Cancer Res* **12**, 6144–6152.

[24] Huang PH, Mukasa A, Bonavia R, Flynn RA, Brewer ZE, Cavenee WK, Furnari FB, and White FM (2007). Quantitative analysis of EGFRvIII cellular signaling networks reveals a combinatorial therapeutic strategy for glioblastoma. *Proc Natl Acad Sci USA* **104**, 12867–12872.

[25] Johns TG, Perera RM, Vernes SC, Vitali AA, Cao DX, Cavenee WK, Scott AM, and Furnari FB (2007). The efficacy of epidermal growth factor receptor–specific antibodies against glioma xenografts is influenced by receptor levels, activation status, and heterodimerization. *Clin Cancer Res* **13**, 1911–1925.

[26] Comer JE, Chopra AK, Peterson JW, and Konig R (2005). Direct inhibition of T-lymphocyte activation by anthrax toxins *in vivo*. *Infect Immun* **73**, 8275–8281.

[27] Jo M, Stolz DB, Esplen JE, Dorko K, Michalopoulos GK, and Strom SC (2000). Cross-talk between epidermal growth factor receptor and c-Met signal pathways in transformed cells. *J Biol Chem* **275**, 8806–8811.

[28] Bachleitner-Hofmann T, Sun MY, Chen CT, Tang L, Song L, Zeng Z, Shah M, Christensen JG, Rosen N, Solit DB, et al. (2008). HER kinase activation confers resistance to MET tyrosine kinase inhibition in MET oncogene–addicted gastric cancer cells. *Mol Cancer Ther* **7**, 3499–3508.

[29] Migliore C and Giordano S (2008). Molecular cancer therapy: can our expectation be MET? *Eur J Cancer* **44**, 641–651.

[30] Narita Y, Nagane M, Mishima K, Huang HJ, Furnari FB, and Cavenee WK (2002). Mutant epidermal growth factor receptor signaling down-regulates p27 through activation of the phosphatidylinositol 3-kinase/Akt pathway in glioblastomas. *Cancer Res* **62**, 6764–6769.

[31] Ziegler DS, Kung AL, and Kieran MW (2008). Anti-apoptosis mechanisms in malignant gliomas. *J Clin Oncol* **26**, 493–500.

[32] Habib AA, Hognason T, Ren J, Stefansson K, and Ratan RR (1998). The epidermal growth factor receptor associates with and recruits phosphatidylinositol 3-kinase to the platelet-derived growth factor beta receptor. *J Biol Chem* **273**, 6885–6891.

[33] Calzolari F, Appolloni I, Tutucci E, Caviglia S, Terrile M, Corte G, and Malatesta P (2008). Tumor progression and oncogene addiction in a PDGF-B–induced model of gliomagenesis. *Neoplasia* **10**, 1373–1382; following 1382.

[34] Luwor RB, Zhu HJ, Walker F, Vitali AA, Perera RM, Burgess AW, Scott AM, and Johns TG (2004). The tumor-specific de2-7 epidermal growth factor receptor (EGFR) promotes cells survival and heterodimerizes with the wild-type EGFR. *Oncogene* **23**, 6095–6104.

[35] Belda-Iniesta C, Carpeno Jde C, Saenz EC, Gutierrez M, Perona R, and Baron MG (2006). Long term responses with cetuximab therapy in glioblastoma multiforme. *Cancer Biol Ther* **5**, 912–914.

[36] Reardon DA. Phase II study of AMG 102, a fully human neutralizing antibody against hepatocyte growth factor/scatter factor, in patients with recurrent glioblastoma multiforme. In: 2008 ASCO Annual Meeting; San Francisco, CA. Abstract no. 2051.

[37] Mathieu V, De Neve N, Le Mercier M, Dewelle J, Gaussin JF, Dehoux M, Kiss R, and Lefranc F (2008). Combining bevacizumab with temozolomide increases the antitumor efficacy of temozolomide in a human glioblastoma orthotopic xenograft model. *Neoplasia* **10**, 1383–1392.

[38] Vredenburgh JJ, Desjardins A, Herndon JE II, Dowell JM, Reardon DA, Quinn JA, Rich JN, Sathornsumetee S, Gururangan S, Wagner M, et al. (2007). Phase II trial of bevacizumab and irinotecan in recurrent malignant glioma. *Clin Cancer Res* **13**, 1253–1259.

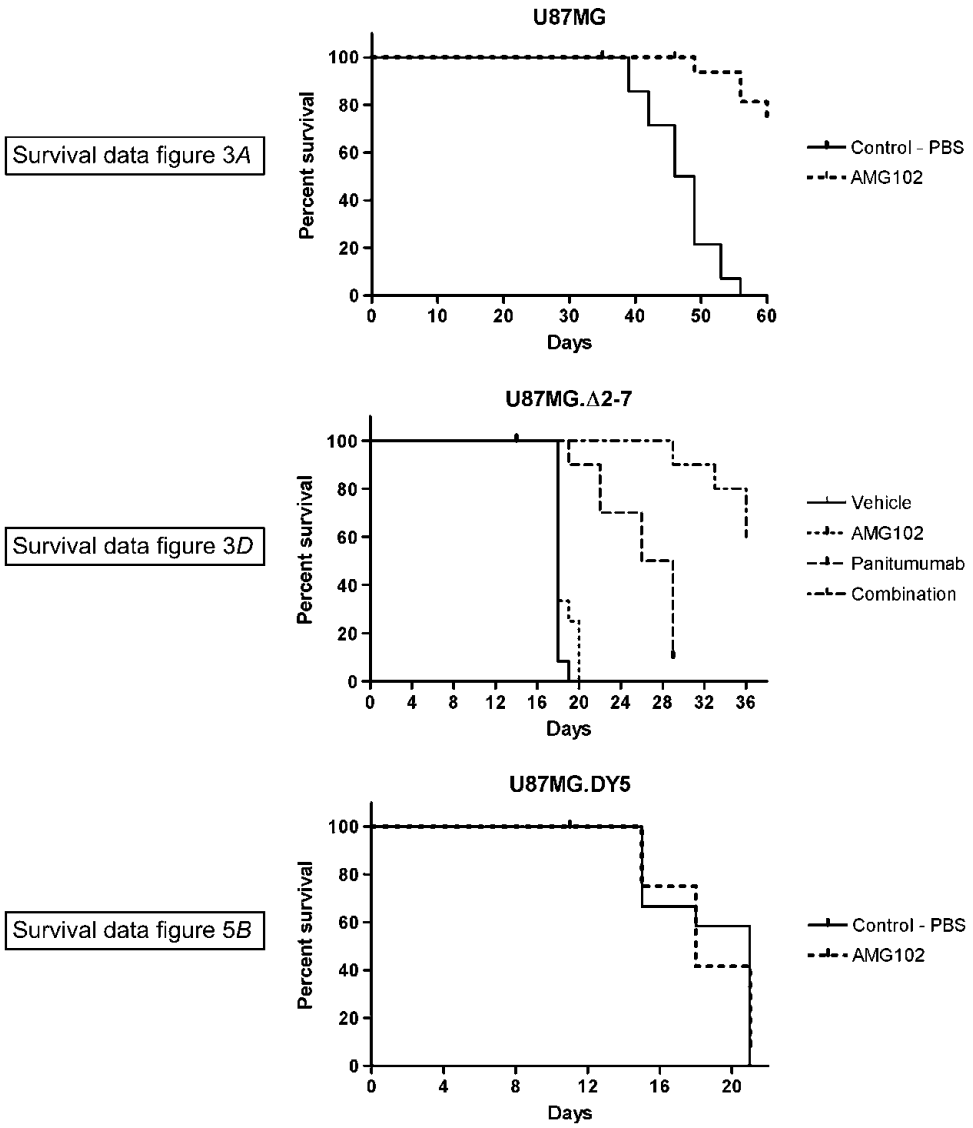

Figure W1. Survival data from xenograft studies. Survival analyses for the therapy studies described in Figures 3, *A* and *D*, and 5*B*. Survival was evaluated using the technique of Kaplan-Meier with comparisons between groups analyzed by log-rank test. A combined end point of moribund condition or tumor volume reaching 1000 mm^3 in mice treated with vehicle.

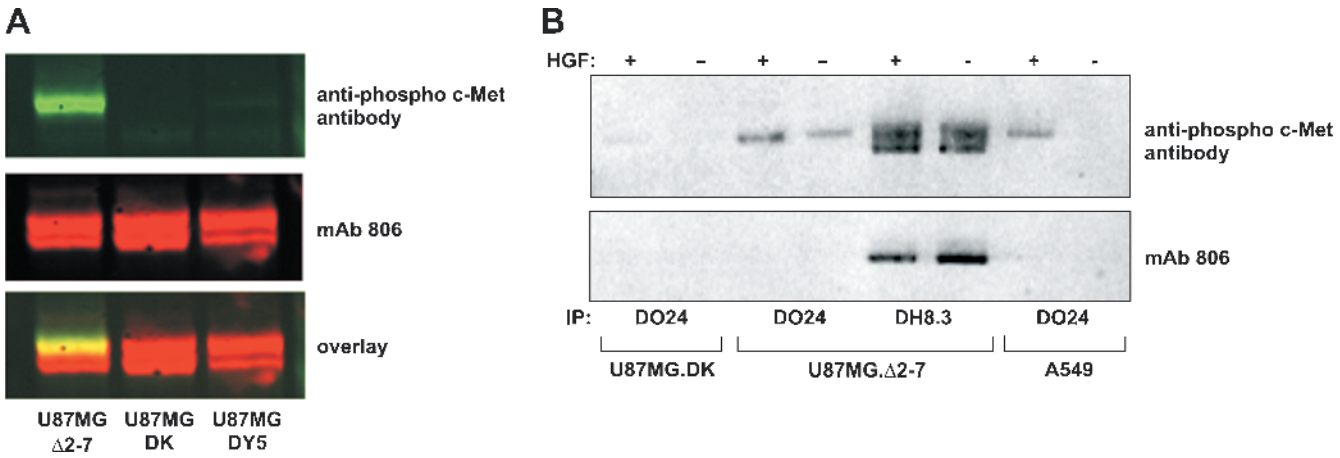

Figure W2. Cross-reactivity between phospho–c-Met antibodies and constitutively active de2-7 EGFR. (A) U87MG.Δ2-7, U87MG.DK, and U87MG.DY5 whole-cell lysates were Western blotted with mAb 806 (anti-EGFR; middle panel) or anti–phospho c-Met (upper panel; rabbit (polyclonal) phosphospecific anti–c-Met [pYpYpY$^{1230/1234/1235}$] from Invitrogen). De2-7 EGFR–related proteins can be seen in all cell lines. In contrast, a p–c-Met band can only be seen in U87MG.Δ2-7. Because the de2-7 EGFR is not phosphorylated in U87MG.DK and U87MG.DY5 cells and because p–c-Met and de2-7 EGFR comigrate (lower panel), it is impossible to determine whether the band seen in the upper panel is p–c-Met or the antibody cross-reacting with de2-7 EGFR. (B) U87MG.Δ2-7 and U87MG.DK cells were immunoprecipitated with DO24 (c-Met–specific) or DH8.3 (de2-7 EGFR–specific) and Western blotted with phospho–c-Met (upper panel) or mAb 806 (lower panel). A549 cells ± HGF were used as a control. As can be clearly seen, the de2-7 EGFR immunoprecipitated by DH8.3 cross-reacted with the anti–p–c-Met antibody. Specific phosphorylation of c-Met could only be observed after immunoprecipitation with DO24. Similar results were obtained using three different phosphospecific c-Met antibodies. Thus, these antibodies cannot be used to determine levels of phosphorylated c-Met by immunohistochemistry in tissues expressing the de2-7 EGFR.